Journal of Medicinal Chemistry Article

J. Med. Chem. **2010,** *53,* 2063–2075 **2063**
DOI: 10.1021/jm9015747

The Amino-Terminus of Angiotensin II Contacts Several Ectodomains of the Angiotensin II Receptor AT_1

Dany Fillion, Guillaume Lemieux, Luta Luse Basambombo, Pierre Lavigne, Gaétan Guillemette, Richard Leduc, and Emanuel Escher*

Department of Pharmacology, Faculty of Medicine and Health Sciences, Université de Sherbrooke, Sherbrooke, QC, Canada J1H 5N4

Received October 23, 2009

G protein-coupled receptors (GPCRs) are the largest family of cell surface receptors and major targets for drug development. Herein, we sought to identify the regions of the human angiotensin II (AngII) type 1 (hAT_1) receptor binding cleft that interact with all positions of the AngII using photoaffinity labeling. We conducted a complete iterative walk-through of the AngII sequence with either *p*-benzoyl-L-phenylalanine (Bpa) or *p*-[3-(trifluoromethyl)-3*H*-diazirin-3-yl]-L-phenylalanine (Tdf) to yield two series of eight photoreactive analogues. Pharmacological properties assessment of these sixteen analogues showed that the CAM receptor has a structure−activity relationship (SAR) more amenable to the amino acid substitutions at positions 1, 2, 3, and 5 of AngII than the WT receptor. Photoaffinity labeling of the CAM receptor with the selected analogues, which exhibit different but complementary photochemical properties, suggested that the AngII amino-terminus resides in a hydrophilic environment and interacts simultaneously with different regions of the hAT_1 receptor, including several ectodomains.

Introduction

GPCRs,[a] also known as heptahelical receptors (7TM receptors), belong to the largest family of integral membrane proteins and are involved in most major physiological processes.[1] They respond to a wide array of stimuli ranging from photons to large glycoproteins to activate signal transduction pathways and, ultimately, cellular responses.[2] In vertebrates, GPCRs are usually divided into five main families based on their sequence and structural similarity: rhodopsin (family A), secretin (family B), glutamate (family C), adhesion, and frizzled/taste2.[3] Overall, the rhodopsin-like GPCRs are the most prominent family member. Structural homology among this family is low and is restricted to a number of highly conserved key residues, suggesting that these residues play an essential role in the integrity of these receptors. In view of their involvement in a broad range of biological functions and the great potential for drug-based therapies, considerable effort has been expended to understand the structural and functional bases of GPCR functions. Large ligands such as glycoprotein hormones are thought to contact the extracellular regions of rhodopsin-like GPCRs close to the membrane surface, whereas smaller ligands such as biogenic amines bind deeper within the space created by the transmembrane domain (TMD) core. Smaller peptides may bind to extracellular regions and TMDs using a combination of both these binding modes.[4−6]

Photoaffinity labeling is a biochemical approach that allows the direct characterization of sites of interaction between a ligand and its related receptor.[7−10] This method is based on a reaction between a photoreactive ligand and a receptor to produce a covalent complex. The photolabeled ligand/receptor complex is submitted to specific proteolysis reactions to determine which region or residue of the receptor has been cross-linked by the photoprobe. The use of both the Bpa and Tdf photoprobe amino acids, which exhibit different but complementary photochemical properties, makes it possible to better characterize the binding cleft of peptidergic GPCRs such as the AT_1 receptor (Figure 1). The AngII octapeptide is the active component of the renin angiotensin aldosterone system. This hormone exerts its diverse effects by interacting with two specifics rhodopsin-like GPCRs, the AT_1 and the AngII type 2 (AT_2) receptors. The vast majority of the physiological effects of this hormone on the cardiovascular, endocrine, and neuronal systems are mediated by the AT_1 receptor canonically coupled to the $G_{q/11}$/phospholipase C/inositol phosphate/cytosolic Ca^{2+} intracellular signaling pathway.[11]

Our previous studies demonstrated that analogues ^{125}I-[Bpa_1]AngII and ^{125}I-[Sar_1,Bpa_3]AngII photolabel the extracellular loop (ECL) 2 of the human AT_1 receptor (hAT_1),[12,13] whereas analogues ^{125}I-[Sar_1,Bpa_8]AngII photolabel various residues located deeper within the TMDs 2, 3, 5, 6, and 7.[12,14−16] In silico molecular modeling incorporating

*To whom correspondence should be addressed. (address) Department of Pharmacology, Faculty of Medicine and Health Sciences, Université de Sherbrooke, 3001−12th Avenue North, Sherbrooke, Québec, Canada, J1H 5N4; (phone) 819-564−5346; (fax) 819-564−5400; (email) Emanuel.Escher@USherbrooke.ca.

[a] Abbreviations: AngII, angiotensin II; AT_1, angiotensin II type 1 receptor; Bpa, *p*-benzoyl-L-phenylalanine; CAM, constitutively active mutant; ECL, extracellular loop; GPCR, G protein-coupled receptor; NT, N-terminal; SAR, structure−activity relationship; Tdf, *p*-[3-(trifluoromethyl)-3*H*-diazirin-3-yl]-L-phenylalanine; TMD, transmembrane domain; WT, wild-type.

Published on Web 02/10/2010

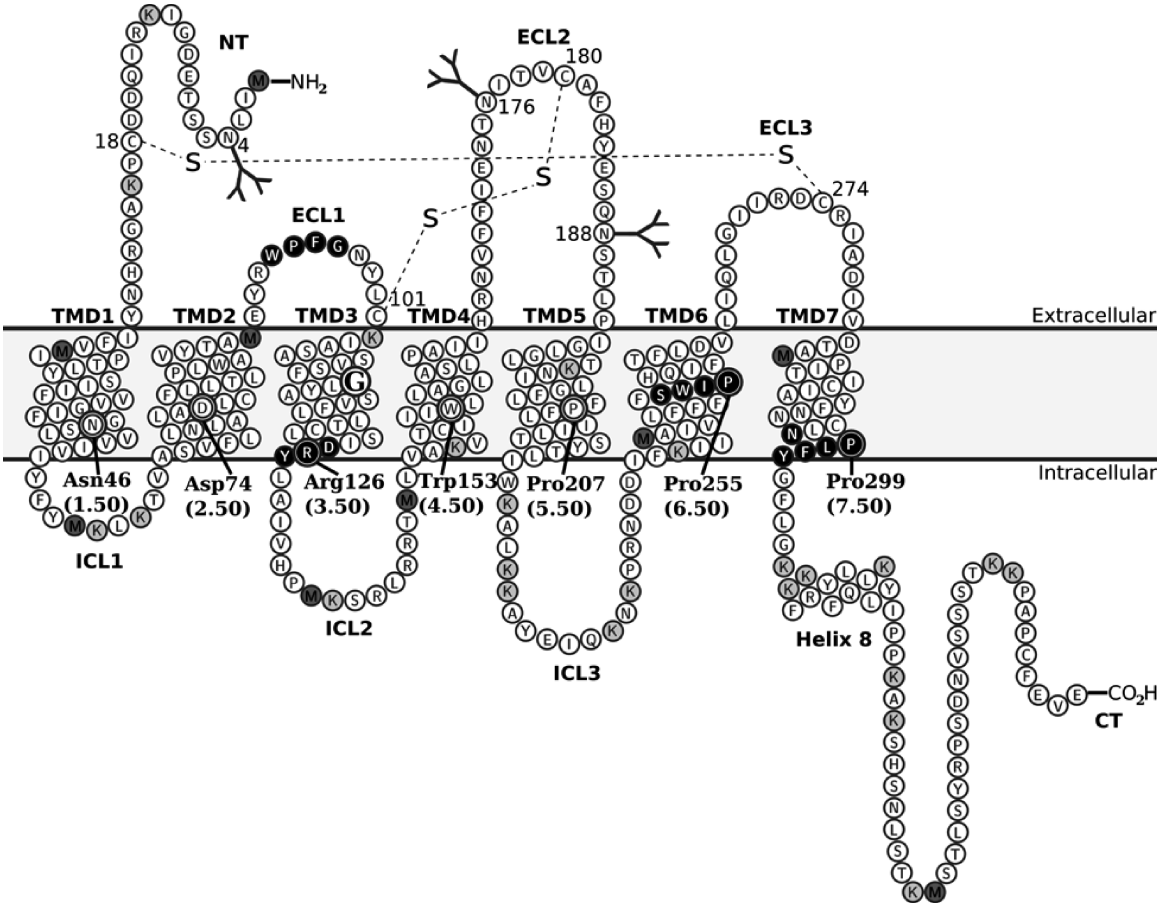

Figure 1. Two-dimensional schematic representation of the primary amino acid structure of the CAM-hAT$_1$ receptor. GPCRs share a common structure composed of seven membrane spanning α-helical segments (transmembrane domains, TMDs) separated by alternating intracellular (ICL) and extracellular (ECL) loop regions, as well as an extracellular N-terminal (NT) and an intracellular C-terminal (CT) extensions. Single-letter amino acid abbreviations are used. The N111G$^{(3.35)}$ mutation inducing constitutive activity is indicated in TMD 3 by a bigger circle and font. The most conserved residues in their respective TMDs in rhodopsin-like GPCRs are represented by black and white circles containing the corresponding letter. These indexed residues are Asn46$^{(1.50)}$, Asp74$^{(2.50)}$, Arg126$^{(3.50)}$, Trp153$^{(4.50)}$, Pro207$^{(5.50)}$, Pro255$^{(6.50)}$, and Pro299$^{(7.50)}$. The three putative *N*-glycosylation sites (Asn4$^{(1.08)}$, Asn176$^{(4.73)}$, and Asn188$^{(5.31)}$), the two disulfide bridges (Cys18$^{(1.22)}$-Cys274$^{(7.25)}$ and Cys101$^{(3.25)}$-Cys180$^{(5.23)}$) as well as the intracellular helix 8 are also shown. Important motifs for receptor structures and functions are indicated by black circles containing a bold white letter. Native Met residues are depicted by bold gray circles containing a bold black M, whereas native Lys residues are represented by light gray circles containing a bold black K.

these experimentally determined ligand/receptor contacts resulted in the development of an evidence-based homology model of the liganded hAT$_1$ receptor complex where the interaction of the AngII carboxyl-terminus with its cognate receptor is practically identical to the crystal structure of the retinal/bovine rhodopsin complex.[16] Nevertheless, the individual interactions of the AngII amino acids positions 2, 4, 5, 6, and 7 with the various regions of the hAT$_1$ receptor remain unresolved. Since the SAR of the AngII/AT$_1$ system is not very permissive toward amino acid substitutions within the AngII octapeptide sequence,[17−20] a receptor model where such substitutions are better tolerated was mandatory.

In the present contribution, we first conducted a complete iterative photoprobe walkthrough of the AngII octapeptide sequence in order to characterize its interactions with the hAT$_1$ receptor. We then used the wild-type (WT) and a CAM of the hAT$_1$ receptor, [N111G]-hAT$_1$ (CAM-hAT$_1$),[21,22] to validate the analogues with pharmacological profiles warranting further investigation. Lastly, we sought to identify the different regions of the hAT$_1$ receptor binding cleft that interact with a given position of the AngII ligand using a photoaffinity labeling approach.

Results

Synthesis of the Radiolabeled Photoreactive AngII Analogues. We synthesized two series of eight radiolabeled photoreactive AngII analogues. For the Bpa-substituted AngII analogue series, we iteratively monoincorporated the Bpa photoprobe amino acid (Chart 1A) in each of the eight positions of the AngII octapeptide sequence to yield analogues **B1** to **B8** (Chart 1B). We also synthesized a Tdf-substituted AngII analogue series using a previously synthesized Tdf photoprobe amino acid[23] (Chart 1A) to produce analogues **T1** to **T8** (Chart 1B). To increase binding affinity, an Asp-to-sarcosin (Sar) modification was performed at position 1 of the peptide sequence.[24] Note that the analogues **B1**, **B3**, **B8**, and **T8** have all been previously described.[12,13,23,24] For photoaffinity labeling experiments, each photoreactive analogue was radiolabeled at Tyr4 with the ^{125}I radioisotope to allow autoradiographic detection of the photolabeled ligand/receptor complexes and its proteolysis products.

Pharmacological Properties of the WT- and CAM-hAT$_1$ Receptors with Respect to the Photoreactive AngII Analogues. To assess the conservation of the structural and functional

Chart 1. Structures of the Photoprobe Amino Acids and Photoreactive AngII Analogues[a]

A)

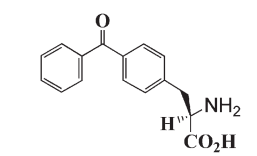

p-Benzoyl-L-Phenylalanine **(Bpa)**

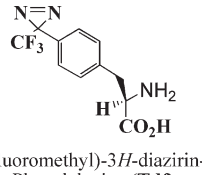

p-[3-(Trifluoromethyl)-3*H*-diazirin-3-yl] -L-Phenylalanine **(Tdf)**

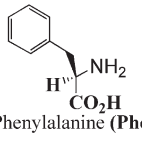

L-Phenylalanine **(Phe)**

B)

AngII:	$H_2N-Asp-Arg-Val-Tyr-Ile-His-Pro-Phe-CO_2H$
[**Bpa$_1$**]AngII **(B1)**:	H_2N-**Bpa**$-Arg-Val-Tyr-Ile-His-Pro-Phe-CO_2H$
[**Tdf$_1$**]AngII **(T1)**:	H_2N-**Tdf**$-Arg-Val-Tyr-Ile-His-Pro-Phe-CO_2H$
[Sar$_1$,**Bpa$_2$**]AngII **(B2)**:	$H_2N-Sar-$**Bpa**$-Val-Tyr-Ile-His-Pro-Phe-CO_2H$
[Sar$_1$,**Tdf$_2$**]AngII **(T2)**:	$H_2N-Sar-$**Tdf**$-Val-Tyr-Ile-His-Pro-Phe-CO_2H$
[Sar$_1$,**Bpa$_3$**]AngII **(B3)**:	$H_2N-Sar-Arg-$**Bpa**$-Tyr-Ile-His-Pro-Phe-CO_2H$
[Sar$_1$,**Tdf$_3$**]AngII **(T3)**:	$H_2N-Sar-Arg-$**Tdf**$-Tyr-Ile-His-Pro-Phe-CO_2H$
[Sar$_1$,**Bpa$_4$**,Tyr$_8$]AngII **(B4)**:	$H_2N-Sar-Arg-Val-$**Bpa**$-Ile-His-Pro-Tyr-CO_2H$
[Sar$_1$,**Tdf$_4$**,Tyr$_8$]AngII **(T4)**:	$H_2N-Sar-Arg-Val-$**Tdf**$-Ile-His-Pro-Tyr-CO_2H$
[Sar$_1$,**Bpa$_5$**]AngII **(B5)**:	$H_2N-Sar-Arg-Val-Tyr-$**Bpa**$-His-Pro-Phe-CO_2H$
[Sar$_1$,**Tdf$_5$**]AngII **(T5)**:	$H_2N-Sar-Arg-Val-Tyr-$**Tdf**$-His-Pro-Phe-CO_2H$
[Sar$_1$,**Bpa$_6$**]AngII **(B6)**:	$H_2N-Sar-Arg-Val-Tyr-Ile-$**Bpa**$-Pro-Phe-CO_2H$
[Sar$_1$,**Tdf$_6$**]AngII **(T6)**:	$H_2N-Sar-Arg-Val-Tyr-Ile-$**Tdf**$-Pro-Phe-CO_2H$
[Sar$_1$,**Bpa$_7$**]AngII **(B7)**:	$H_2N-Sar-Arg-Val-Tyr-Ile-His-$**Bpa**$-Phe-CO_2H$
[Sar$_1$,**Tdf$_7$**]AngII **(T7)**:	$H_2N-Sar-Arg-Val-Tyr-Ile-His-$**Tdf**$-Phe-CO_2H$
[Sar$_1$,**Bpa$_8$**]AngII **(B8)**:	$H_2N-Sar-Arg-Val-Tyr-Ile-His-Pro-$**Bpa**$-CO_2H$
[Sar$_1$,**Tdf$_8$**]AngII **(T8)**:	$H_2N-Sar-Arg-Val-Tyr-Ile-His-Pro-$**Tdf**$-CO_2H$

[a] (A) Chemical structures of the *p*-benzoyl-L-phenylalanine (Bpa) and of the *p*-[3-(trifluoromethyl)-3*H*-diazirin-3-yl]-L-phenylalanine (Tdf) photoprobe amino acids compared to the natural Phe amino acid. Note that these three amino acids are quite biosteric. (B) Primary amino acid structure of the AngII peptide and the photoreactive AngII analogues. The Bpa and Tdf photoprobe are indicated in bold within the name and sequence of the peptide. For photoaffinity labeling experiments, each photoreactive analogue was radiolabeled at Tyr4 with the ^{125}I radioisotope (not represented). Since Tyr is the ^{125}I radioisotope incorporation site, Phe was substituted for Tyr at position **8** for analogues **B4** and **T4**. Analogues **B1**, **B3**, **B8**, and **T8** have all been previously described.[12,13,23,24]

integrity of the WT- and CAM-hAT$_1$ receptors, pharmacological parameters describing the equilibrium dissociation constant (K_i) as well as the biological properties (ligand-induced inositol-1-monophosphate (IP_1) production levels) were evaluated for each photoreactive analogues. In the binding affinity assays (Table 1), for the WT-hAT$_1$ receptor, analogues **B3**, **T3**, **B8**, and **T8** displayed high affinities that were equivalent to that of the native AngII peptide. Analogues **B1**, **T1**, **B2**, and **T2** exhibited reduced affinities, whereas analogues **B4**, **T4**, **B5**, **T5**, **B6**, **T6**, **B7**, and **T7** presented much lower affinities. For the CAM-hAT$_1$ receptor, analogues **B1**, **T1**, **B2**, **T2**, **B3**, **T3**, **B5**, **T5**, **B8**, and **T8** retained high affinities similar to that of the native AngII peptide. Analogues **B6**, **T6**, **B7**, and **T7** displayed reduced affinities, while analogues **B4** and **T4** exhibited much lower affinities. We thus selected the photoreactive analogues that maintained AngII-like binding affinities toward both receptors in order to characterize their capacities to produce levels of IP1. These analogues were those substituted at positions 1, 2, 3, and 8 for both receptors and at position 5 for the CAM-hAT$_1$ receptor alone.

In the biological activity assays (Table 2), with the WT-hAT$_1$ receptor, analogues **B1**, **T1**, **B2**, and **T2** elicited IP_1 production levels comparable to that of the native AngII peptide, which was indicative of the full agonist character of the analogues substituted at positions 1 and 2. Analogues **B3**, **T3**, and **T8** had reduced levels of IP_1 consistent with their partial agonist nature. Analogue **B8** displayed antagonist properties, with levels of IP1 equivalent to the basal level of the WT-hAT$_1$ receptor. With the CAM-hAT$_1$ receptor, analogues **B1**, **T1**, **B2**, **T2**, **B3**, **T3**, **B5**, and **T5** produced IP_1 levels equivalent to that of the native AngII peptide, which was indicative of the full agonist character of analogues substituted at positions 1, 2, 3, and 5. Analogues **T8** showed reduced levels of IP_1 consistent with their partial agonist nature. Analogue **B8** exhibited neutral antagonist

properties since its level of IP_1 were similar to the basal levels of the CAM-hAT_1 receptor.

Since the CAM-hAT_1 receptor preserved nearly native pharmacological properties (K_i and IP_1 production levels) for **B1**, **T1**, **B2**, **T2**, **B3**, **T3**, **B5**, and **T5**, photoaffinity labeling studies were continued on this receptor model alone.

Table 1. Binding Affinities of the WT- and CAM-hAT_1 Receptors for the Photoreactive AngII Analogues[a]

AngII substituted position	photoreactive AngII analogue	K_i (nM) WT-hAT_1	K_i (nM) CAM-hAT_1
	AngII	0.9 ± 0.2	0.5 ± 0.1
1	[**Bpa_1**]AngII (**B1**)	19.4 ± 3.7	0.8 ± 0.2
	[**Tdf_1**]AngII (**T1**)	26.4 ± 7.1	0.7 ± 0.3
2	[Sar_1,**Bpa_2**]AngII (**B2**)	18.3 ± 3.4	0.6 ± 0.2
	[Sar_1,**Tdf_2**]AngII (**T2**)	24.7 ± 6.7	0.4 ± 0.2
3	[Sar_1,**Bpa_3**]AngII (**B3**)	0.7 ± 0.2	0.4 ± 0.1
	[Sar_1,**Tdf_3**]AngII (**T3**)	1.3 ± 0.3	0.3 ± 0.1
4	[Sar_1,**Bpa_4**,Tyr_8]-AngII (**B4**)	≥500	≥250
	[Sar_1,**Tdf_4**,Tyr_8]-AngII (**T4**)	≥500	≥250
5	[Sar_1,**Bpa_5**]AngII (**B5**)	≥250	0.7 ± 0.2
	[Sar_1,**Tdf_5**]AngII (**T5**)	≥250	0.5 ± 0.2
6	[Sar_1,**Bpa_6**]AngII (**B6**)	≥500	31.6 ± 5.8
	[Sar_1,**Tdf_6**]AngII (**T6**)	≥500	58.2 ± 13.9
7	[Sar_1,**Bpa_7**]AngII (**B7**)	≥500	12.8 ± 4.1
	[Sar_1,**Tdf_7**]AngII (**T7**)	≥500	3.8 ± 0.9
8	[Sar_1,**Bpa_8**]AngII (**B8**)	0.8 ± 0.2	0.6 ± 0.2
	[Sar_1,**Tdf_8**]AngII (**T8**)	0.9 ± 0.3	0.7 ± 0.3

[a] Binding affinities (K_i) were obtained by heterologous competition binding using ^{125}I-[Sar_1,Ile_8]AngII (Sarile) as the radioactive tracer, which is displaced by increasing concentrations of the indicated cold ligand. Binding assays were run in cell membrane preparations of transiently transfected COS-7 cells. See Experimental section for further details. The means ± SD shown are for at least three independent experiments, each with duplicate determinations. The K_i values were determined from the IC_{50} values using the Cheng-Prusoff equation: $K_i = IC_{50}/(1 + ([Tracer]/K_d))$, where K_i is the equilibrium dissociation constant of a ligand determined in inhibition studies, IC_{50} is the molar concentration of an unlabeled ligand that inhibits the binding of a radioligand by 50%, [Tracer] is the molar concentration of radioligand used, and K_d is the equilibrium dissociation constant of the tracer determined directly in a binding assay using a labeled form of the ligand and under the same experimental conditions used in the competition experiment.

Photoaffinity Labeling of the CAM-hAT_1 Receptor by the Photoreactive AngII Analogues. The specificity of the photolabeling process of the selected analogues ^{125}I-**B1**, ^{125}I-**B2**, ^{125}I-**T2**, ^{125}I-**B3**, ^{125}I-**T3**, ^{125}I-**B5**, and ^{125}I-**T5** was validated on the CAM-hAT_1 receptor by the complete abolition of the labeling by 1 mM of AngII (Figure 2A, lanes 2, 6, 10, 14, 18, 22, 26). Each of those ligand/receptor interactions was specific and decreased in a dose-dependent manner in the presence of AngII (data not shown). These photoreactive analogues specifically labeled the CAM-hAT_1 receptor, which diffusely migrated on SDS-PAGE gels as a broad glycoprotein band with an apparent molecular mass of 100−250 kDa (Figure 2A, lanes 3, 7, 11, 15, 19, 23, 27), as previously described.[12−14,25,26] All these analogues had good (^{125}I-**B1**, ^{125}I-**T2**, ^{125}I-**B5**, and ^{125}I-**T5**) to excellent (^{125}I-**B2**, ^{125}I-**B3**, and ^{125}I-**T3**) photoaffinity labeling yields of covalent incorporation with the CAM-hAT_1 receptor, except for analogue ^{125}I-**T1** whose low yield prevented further investigation. The other photoreactive analogues had good (^{125}I-**B8** and ^{125}I-**T8**) to low (^{125}I-**B7** and ^{125}I-**T7**) or extremely low (^{125}I-**B4**, ^{125}I-**T4**, ^{125}I-**B6**, and ^{125}I-**T6**) photolabeling yields with the CAM-hAT_1 receptor (Table 3).

Determination of the CAM-hAT_1 Receptor Regions Photolabeled by the Photoreactive AngII Analogues. To identify the CAM-hAT_1 receptor regions photolabeled by the photoreactive analogues, we cleaved the relevant photolabeled ligand/receptor complexes with cyanogen bromide (CNBr), with or without peptide-*N*-glycosidase F peptide-N^4-(acetyl-β-glucosaminyl)-asparagine amidase (PNGase F) deglycosylation, and also digested them with endoproteinase Lys-C (endoLys-C).

CNBr Cleavages of the ^{125}I-B1, ^{125}I-B2, ^{125}I-T2, ^{125}I-B3, ^{125}I-T3, ^{125}I-B5, and ^{125}I-T5 Photolabeled Receptor Complexes. We first cleaved the partially purified 100−250 kDa glycoprotein band of the ^{125}I-**B1**, ^{125}I-**B2**, ^{125}I-**T2**, ^{125}I-**B3**, ^{125}I-**T3**, ^{125}I-**B5**, or ^{125}I-**T5** photolabeled receptor complexes with CNBr. This chemical reactant specifically hydrolyzes peptide bonds at the carboxylic side of Met residues. The CNBr products of the photolabeled receptor complexes appear as sharp, nondiffuse protein bands on SDS-PAGE

Table 2. Ligand−Induced Inositol-1-Monophosphate Production by the WT- and CAM-hAT_1 Receptor[a]

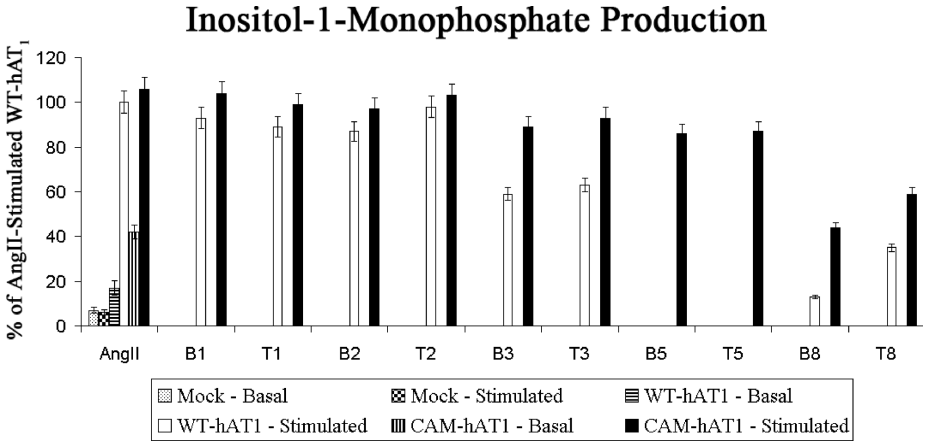

[a] Basal (vehicle) and stimulated (1×10^{-6} M final concentration of AngII analogue) inositol-1-monophosphate (IP_1) production were induced in transiently transfected COS-7 cells for 30 minutes at 37 °C in a 5% [v/v] CO_2 atmosphere. Each condition was run in triplicate, and parallel wells were used to measure receptor expression. IP_1 levels were adjusted based on receptor expression levels. See Experimental section for further details. The means ± SD shown are for three independent experiments, each with triplicate determinations.

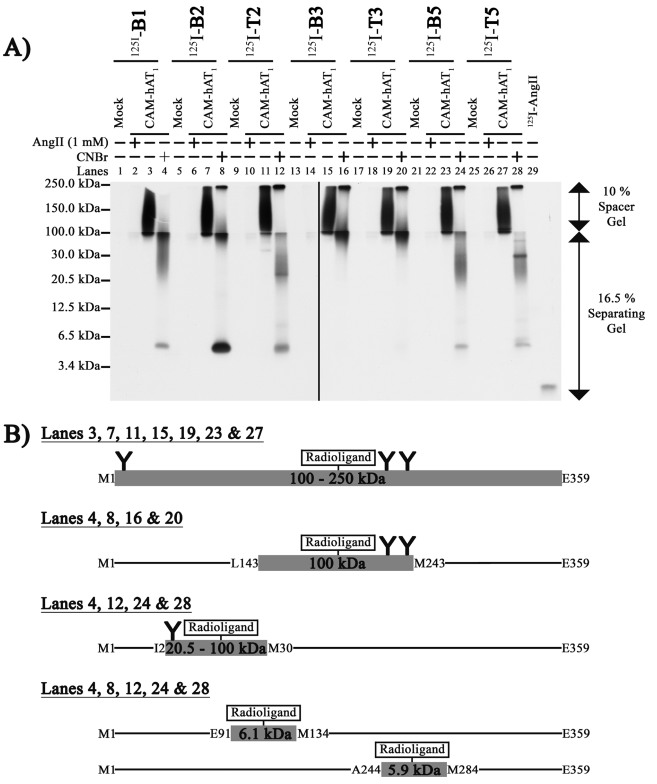

Figure 2. (A) Photoaffinity labeling and glycosylation fragmentation patterns of the CAM-hAT$_1$ receptor photolabeled by the photoreactive AngII analogues. Analogues ^{125}I-**B1**, ^{125}I-**B2**, ^{125}I-**T2**, ^{125}I-**B3**, ^{125}I-**T3**, ^{125}I-**B5**, and ^{125}I-**T5** were individually photolabeled on the CAM-hAT$_1$ receptor. The resulting photolabeled ligand/receptor complexes and proteolysis products were then analyzed on SDS-PAGE gels followed by autoradiography. Photolabeling of the mock (lanes 1, 5, 9, 13, 17, 21, 25) as well as the CAM-hAT$_1$ receptor in the presence (lanes 2, 6, 10, 14, 18, 22, 26) or in the absence (lanes 3, 7, 11, 15, 19, 23, 27) of 1 mM AngII and CNBr products of the Met cleavage of the photolabeled ligand/receptor complexes (lanes 4, 8, 12, 16, 20, 24, 28) are shown. Each ligand/receptor interaction was specific and decreased in a dose-dependent manner in the presence of AngII (data not shown). Low molecular mass protein standards were used to determine apparent molecular masses. See Experimental section for further details. These results are representative of at least four independent experiments. (B) Schematic glycosylation fragmentation patterns of the CAM-hAT$_1$ receptor photolabeled by the photoreactive AngII analogues. Putative photolabeled CAM-hAT$_1$ receptor regions are depicted as thick gray bars, and the photoreactive AngII analogue as a box with "Radioligand" inside. Single-letter amino acid abbreviations are used with position numbers. The calculated molecular masses of the photolabeled regions are shown as the thick gray bars and include the molecular mass of the photolabeled radioligand. The three putative *N*-glycosylation sites are indicated by "Y". All the analogues, i.e., ^{125}I-**B1**, ^{125}I-**B2**, ^{125}I-**T2**, ^{125}I-**B3**, ^{125}I-**T3**, ^{125}I-**B5**, and ^{125}I-**T5**, specifically photolabeled a broad glycosylated protein band with ambiguous apparent molecular mass of 100−250 kDa (glycosylated M1$^{(1.05)}$-E359$^{(7.110)}$, glycosylated CAM-hAT$_1$). Analogues ^{125}I-**B1**, ^{125}I-**B2**, ^{125}I-**B3**, and ^{125}I-**T3** photolabeled a glycoprotein band with ambiguous apparent molecular mass of 100 kDa (diglycosylated L143$^{(4.40)}$-M243$^{(6.38)}$). Analogues ^{125}I-**B1**, ^{125}I-**T2**, ^{125}I-**B5**, and ^{125}I-**T5** also photolabeled a diffuse glycoprotein band with an ambiguous apparent molecular mass of 20.5−100 kDa (monoglycosylated I2$^{(1.06)}$-M30$^{(1.34)}$). Analogues ^{125}I-**B1**, ^{125}I-**B2**, ^{125}I-**T2**, ^{125}I-**B5**, and ^{125}I-**T5** photolabeled a sharp nonglycosylated protein band with an apparent molecular mass of 6.0 kDa (E91$^{(2.67)}$-M134$^{(3.58)}$, theoretical molecular mass of 6.1 kDa and/or A244$^{(6.39)}$-M284$^{(7.35)}$, theoretical molecular mass of 5.9 kDa).

Table 3. Photoaffinity Labeling Yields of Covalent Incorporation of the Photoreactive AngII Analogues into the CAM-hAT$_1$ Receptor[a]

substituted position	photoreactive AngII analogue	photoaffinity labeling yield of CAM-hAT$_1$ (%)	difference in photoaffinity labeling yield (fold)
1	[**Bpa$_1$**]AngII (**B1**)	38 ± 4	5.4
	[**Tdf$_1$**]AngII (**T1**)	7 ± 1	
2	[Sar$_1$,**Bpa$_2$**]AngII (**B2**)	89 ± 6	4.0
	[Sar$_1$,**Tdf$_2$**]AngII (**T2**)	22 ± 2	
3	[Sar$_1$,**Bpa$_3$**]AngII (**B3**)	61 ± 5	not significant
	[Sar$_1$,**Tdf$_3$**]AngII (**T3**)	58 ± 5	
4	[Sar$_1$,**Bpa$_4$**,Tyr$_8$]AngII (**B4**)	not applicable	
	[Sar$_1$,**Tdf$_4$**,Tyr$_8$]AngII (**T4**)		
5	[Sar$_1$,**Bpa5**]AngII (**B5**)	36 ± 5	not significant
	[Sar$_1$,**Tdf$_5$**]AngII (**T5**)	27 ± 4	
6	[Sar$_1$,**Bpa$_6$**]AngII (**B6**)	not applicable	
	[Sar$_1$,**Tdf$_6$**]AngII (**T6**)		
7	[Sar$_1$,**Bpa$_7$**]AngII (**B7**)	not applicable	
	[Sar$_1$,**Tdf$_7$**]AngII (**T7**)		
8	[Sar$_1$,**Bpa$_8$**]AngII (**B8**)	39 ± 5	not significant
	[Sar$_1$,**Tdf$_8$**]AngII (**T8**)	43 ± 5	

[a] Photolabeling yields were calculated from the percentage ratio of radioactivity corresponding to photolabeled ligand/receptor complexes to the related specific binding observed before the photoaffinity labeling. The means ± SD shown are for at least three independent experiments.

gels in the case of nonglycosylated protein fragments or as diffuse protein bands with ambiguous apparent molecular masses in the case of glycoprotein fragments.[27,28] The CNBr-treated ^{125}I-**B1**, ^{125}I-**B2**, ^{125}I-**T2**, ^{125}I-**B5**, and ^{125}I-**T5** photolabeled receptor complexes migrated as a sharp, nonglycosylated protein band with an apparent molecular mass of 6.0 kDa (Figure 2A, lanes 4, 8, 12, 24, 28). Potential photolabeled hAT$_1$ receptor candidate regions (Figure 2B) were the Glu91$^{(2.67)}$-Met134$^{(3.58)}$ region (calculated molecular mass of 6.1 kDa) and the Ala244$^{(6.39)}$-Met284$^{(7.35)}$ region (calculated molecular mass of 5.9 kDa). The CNBr-cleaved ^{125}I-**B1**, ^{125}I-**T2**, ^{125}I-**B5**, and ^{125}I-**T5** photolabeled receptor complexes generated a diffuse glycoprotein band with an ambiguous apparent molecular mass of 20.5−100 kDa (Figure 2A, lanes 4, 12, 24, 28), while the ^{125}I-**B1**, ^{125}I-**B2**, ^{125}I-**B3**, and ^{125}I-**T3** photolabeled receptor complexes produced a glycoprotein band with an ambiguous apparent molecular mass of 100 kDa (Figure 2A, lanes 4, 8, 16, 20). CNBr cleavage of the hAT$_1$ receptor would theoretically yield two glycosylated candidates, namely, the monoglycosylated Ile2$^{(1.06)}$-Met30$^{(1.34)}$ region and the diglycosylated Leu143$^{(4.40)}$-Met243$^{(6.38)}$ region (Figure 2B).

PNGase F Deglycosylations of the ^{125}I-B1, ^{125}I-B2, ^{125}I-T2, ^{125}I-B3, ^{125}I-T3, ^{125}I-B5, and ^{125}I-T5 Photolabeled Receptor Complexes. To further characterize the glycosylated CAM-hAT$_1$ receptor regions photolabeled by the photoreactive analogues, the appropriate CNBr-treated photolabeled receptor complexes were partially purified, and radioactive glycoprotein bands with apparent molecular masses greater than 12.5 kDa were deglycosylated using PNGase F. This enzyme specifically hydrolyzes all types of *N*-glycan chains bound to Asn. The partially purified 20.5−100 kDa protein band of the ^{125}I-**B1**, ^{125}I-**T2**, ^{125}I-**B5**, and ^{125}I-**T5** photolabeled receptor complexes and the 100 kDa protein band of the ^{125}I-**B1**, ^{125}I-**B2**, ^{125}I-**B3**, and ^{125}I-**T3** photolabeled receptor complexes were incubated in the absence (Figure 3A, lanes 1, 2, 4, 6, 8, 10, 12, 14) or presence (Figure 3A, lanes 3, 5, 7, 9, 11, 13, 15) of PNGase F. The

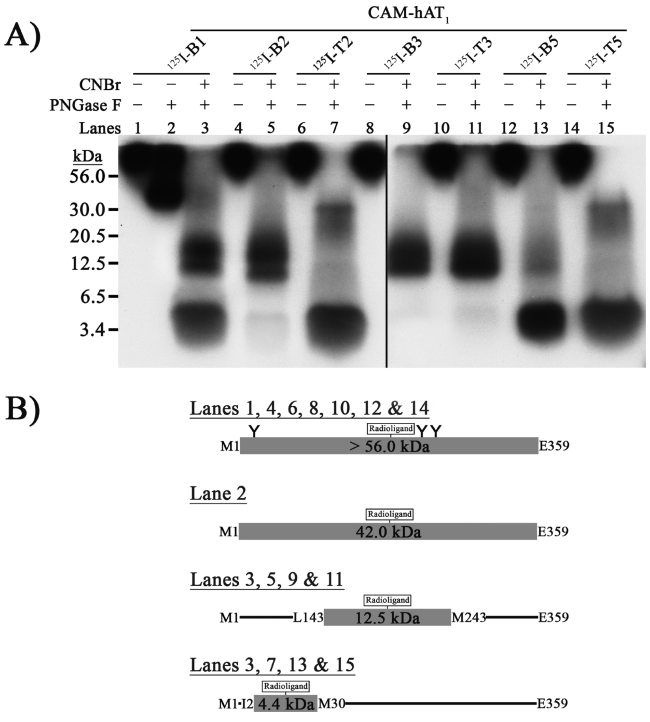

Figure 3. Determination of the glycosylated CAM-hAT$_1$ receptor regions photolabeled by the photoreactive AngII analogues. (A) CNBr cleavage of Met followed by PNGase F deglycosylation of the photolabeled ligand/receptor complexes. Refer to Figure 2A legend. The CNBr products of cleavage of the photolabeled ligand/receptor complexes (see Figure 2A, lanes 4, 8, 12, 16, 20, 24, 28) were partially purified, and the radioactive glycoprotein bands showing an apparent molecular masses greater than 12.5 kDa were incubated in the absence (lanes 1, 4, 6, 8, 10, 12, 14) or presence (lanes 3, 5, 7, 9, 11, 13, 15) of PNGase F. Photolabeled ligand/receptor complexes were also incubated solely in the presence of PNGase F (see lane 2 for a representative example). The results are representative of at least four independent experiments. (B) Schematic fragmentation patterns of the deglycosylated CAM-hAT$_1$ receptor regions photolabeled by the photoreactive AngII analogues. Refer to Figure 2B legend. All the analogues, i.e., ^{125}I-**B1**, ^{125}I-**B2**, ^{125}I-**T2**, ^{125}I-**B3**, ^{125}I-**T3**, ^{125}I-**B5**, and ^{125}I-**T5**, photolabeled a glycoprotein band with ambiguous apparent molecular mass greater than 56 kDa (glycosylated M1$^{(1.05)}$-E359$^{(7.110)}$, glycosylated CAM-hAT$_1$). Analogue ^{125}I-**B1**, as a representative example, photolabeled a protein band with an apparent molecular mass of 45 kDa (deglycosylated M1$^{(1.05)}$-E359$^{(7.110)}$, deglycosylated CAM-hAT$_1$, theoretical molecular mass of 42 kDa). Analogues ^{125}I-**B1**, ^{125}I-**B2**, ^{125}I-**B3**, and ^{125}I-**T3** photolabeled a protein band with an apparent molecular mass of 12.5 kDa (deglycosylated L143$^{(4.40)}$-M243$^{(6.38)}$, theoretical molecular mass of 12.5 kDa). Analogues ^{125}I-**B1**, ^{125}I-**T2**, ^{125}I-**B5**, and ^{125}I-**T5** photolabeled a protein band with an apparent molecular mass of 4.5 kDa (deglycosylated I2$^{(1.06)}$-M30$^{(1.34)}$, theoretical molecular mass of 4.4 kDa).

PNGase F-cleaved ^{125}I-**B1**, ^{125}I-**T2**, ^{125}I-**B5**, and ^{125}I-**T5** photolabeled receptor complexes migrated as a protein band with an apparent molecular mass of 4.5 kDa, confirming that the Ile2$^{(1.06)}$-Met30$^{(1.34)}$ region (calculated molecular mass of 4.4 kDa) was the only candidate (Figure 3B). This region encompasses the NT of the hAT$_1$ receptor. The PNGase F-treated ^{125}I-**B1**, ^{125}I-**B2**, ^{125}I-**B3**, and ^{125}I-**T3** photolabeled receptor complexes generated a protein band with an apparent molecular mass of 12.5 kDa, confirming that the Leu-143$^{(4.40)}$-Met243$^{(6.38)}$ region (calculated molecular mass of 12.5 kDa) was the only candidate (Figure 3B). This region encompasses the TMD 4, ECL 2, TMD 5, and ICL 3 of the hAT$_1$ receptor.

EndoLys-C Digestions of the ^{125}I-B1, ^{125}I-B2, ^{125}I-T2, ^{125}I-B5, and ^{125}I-T5 Photolabeled Receptor Complexes. We previously showed (Figure 2) that the CNBr cleavage of the ^{125}I-**B1**, ^{125}I-**B2**, ^{125}I-**T2**, ^{125}I-**B5**, and ^{125}I-**T5** photolabeled receptor complexes generated a sharp, nonglycosylated protein band with an apparent molecular mass of 6.0 kDa, which could be the Glu91$^{(2.67)}$-Met134$^{(3.58)}$ and/or Ala244$^{(6.39)}$-Met284$^{(7.35)}$ regions. To discriminate between those two candidate regions, we digested the appropriate photolabeled receptor complexes with endoLys-C. This enzyme is a serine protease that specifically hydrolyzes amide, ester, and peptide bonds at the carboxylic side of Lys residues. The partially purified 100−250 kDa protein band of the ^{125}I-**B1**, ^{125}I-**B2**, ^{125}I-**T2**, ^{125}I-**B5**, and ^{125}I-**T5** photolabeled receptor complexes was incubated in the absence (Figure 4A, lanes 1, 3, 5, 7, 9) or presence (Figure 4A, lanes 2, 4, 6, 8, 10) of endoLys-C. The endoLys-C-treated ^{125}I-**B5** and ^{125}I-**T5** photolabeled receptor complexes migrated as a protein band with an apparent molecular mass of 6.0 kDa, which indicated that the Thr61$^{(2.37)}$-Lys102$^{(3.26)}$ (calculated molecular mass of 5.9 kDa) and/or Ala21$^{(1.25)}$-Lys58$^{(1.62)}$ region(s) (calculated molecular mass of 5.4 kDa) were the only candidate(s) (Figure 4B). Given the regions previously identified by CNBr cleavage (i.e., Glu91$^{(2.67)}$-Met134$^{(3.58)}$), the only matching candidate was the Glu91$^{(2.67)}$-Lys102$^{(3.26)}$ region (Scheme 1). This region encompasses the ECL 1 of the hAT$_1$ receptor. The endoLys-C-cleaved ^{125}I-**B1**, ^{125}I-**B2**, and ^{125}I-**T2** photolabeled receptor complexes generated a protein band with an apparent molecular mass of 9.5 kDa, pointing to the Ile241$^{(6.36)}$-Lys307$^{(7.58)}$ region (calculated molecular mass of 8.9 kDa) as the only candidate (Figure 4B). Given the regions previously identified by the CNBr cleavage (i.e., Ala244$^{(6.39)}$-Met284$^{(7.35)}$), the only matching candidate was the Ala244$^{(6.39)}$-Met284$^{(7.35)}$ region (Scheme 1). This region encompasses the TMD 6, ECL 3, and the upper part of the TMD 7 of the hAT$_1$ receptor.

Discussion

The first aim of the present study was to determine whether the WT- or the CAM-hAT$_1$ receptor had a SAR more amenable to amino acid substitution of the AngII octapeptide sequence in order to characterize the topology of the AngII-binding cleft using a photoaffinity labeling approach. Our results (Tables 1 and 2) demonstrated that the CAM-hAT$_1$ receptor was a more permissive system model than the WT receptor with regards to the amino acid substitutions at positions 1, 2, 3, and 5 of the AngII octapeptide sequence. The aromaticity and bulkiness of the side chains of the Bpa and Tdf photoprobes as well as the strong electronegative nature of the CF_3 group of the Tdf did not significantly alter the binding affinities of the CAM receptor. This is in sharp contrast with the major affinity losses observed with the WT receptor. To our knowledge, it is the first time that a SAR is sufficiently tolerant to allow such an extensive structural characterization of the binding cleft of a rhodopsin-like peptidergic CAM-GPCR using a photoaffinity labeling approach.

For the WT-hAT$_1$ receptor, the Asp1 and Arg2 amino acids of the AngII amino-terminus are important for binding affinity and duration of action, but are not essential for biological activity;[17−20] AngIII (Ang2−8) is equipotent to AngII on the AT$_1$ receptor.[29] Moreover, the biological activities of the AngII peptide have been reported to be dependent

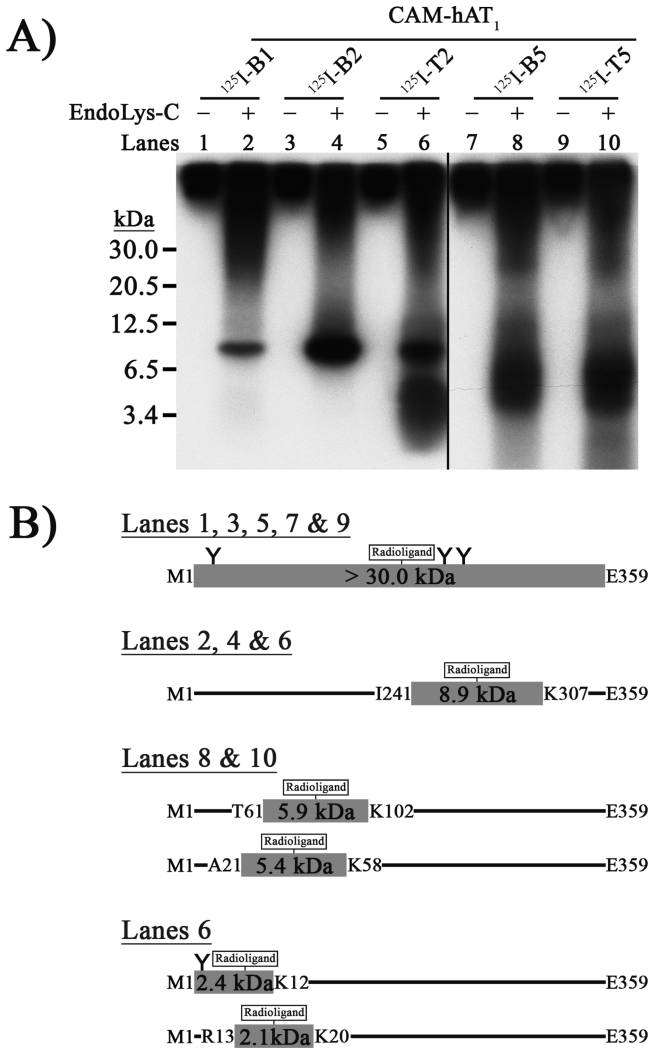

Figure 4. Determination of the unglycosylated CAM-hAT$_1$ receptor regions photolabeled by the photoreactive AngII analogues. (A) EndoLys-C digestions of the photolabeled ligand/receptor complexes. Refer to Figure 2A legend, except for analogues ^{125}I-**B3** and ^{125}I-**T3**. The photolabeled ligand/receptor complexes were incubated in the absence (lanes 1, 3, 5, 7, 9) or presence (lanes 2, 4, 6, 8, 10) of endoLys-C. The results are representative of at least three independent experiments. (B) Schematic fragmentation patterns of the unglycosylated CAM-hAT$_1$ receptor regions photolabeled by the photoreactive AngII analogues. Refer to Figure 3B legend, except for analogues ^{125}I-**B3** and ^{125}I-**T3**. Analogues ^{125}I-**B1**, ^{125}I-**B2**, ^{125}I-**T2**, ^{125}I-**B5**, and ^{125}I-**T5** photolabeled a glycoprotein band with ambiguous apparent molecular mass greater than 30 kDa (glycosylated M1$^{(1.05)}$-E359$^{(7.110)}$, CAM-hAT$_1$). Analogues ^{125}I-**B1**, ^{125}I-**B2**, and ^{125}I-**T2** photolabeled a protein band with an apparent molecular mass of 9.5 kDa (I241$^{(6.36)}$-K307$^{(7.58)}$, theoretical molecular mass of 8.9 kDa). Analogues ^{125}I-**B5** and ^{125}I-**T5** photolabeled a protein band with an apparent molecular mass of 6.0 kDa (T61$^{(2.37)}$-K102$^{(3.26)}$, theoretical molecular mass of 5.9 kDa and/or A21$^{(1.25)}$-K58$^{(1.62)}$, theoretical molecular mass of 5.4 kDa). Analogue ^{125}I-**T2** photolabeled a protein band with an apparent molecular mass of 3.0 kDa (M1$^{(1.05)}$-K12$^{(1.16)}$, theoretical molecular mass of 2.4 kDa and/or R13$^{(1.17)}$-K20$^{(1.24)}$, theoretical molecular mass of 2.1 kDa).

on the Arg2, Tyr4, His6, and Phe8 amino acid side chains as well as the negatively charged carboxyl terminus,[17−20] which together may form a charge relay system.[30−32] The other amino acids, Val3, Ile5, and Pro7, likely are determinants of the AT$_1$ receptor-bound conformation of the AngII ligand.[17−20]

Scheme 1. Schematic Summary of the CAM-hAT$_1$ Receptor Regions Photolabeled by the Photoreactive AngII Analogues[a]

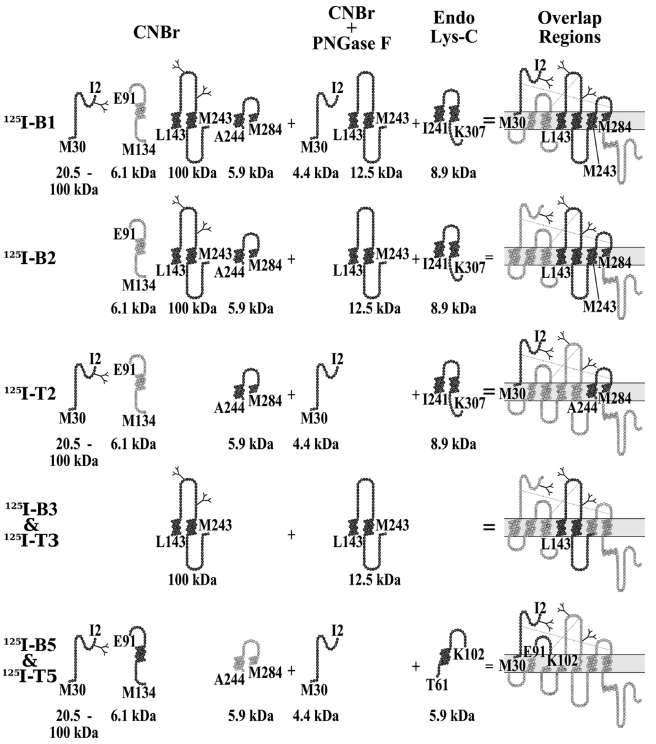

[a] The various chemical and enzymatic agents used as well as the resulting overlapped receptor regions are illustrated horizontally at the top of the figure. The different photoreactive AngII analogues employed are illustrated vertically on the left. Single letter amino acid abbreviations are used with position numbers. The three putative *N*-glycosylation sites (Asn4$^{(1.08)}$, Asn176$^{(4.73)}$, and Asn188$^{(5.31)}$) and the two disulfide bridges (Cys18$^{(1.22)}$-Cys274$^{(7.25)}$ and Cys101$^{(3.25)}$-Cys180$^{(5.23)}$) are shown. All the putative photolabeled CAM-hAT$_1$ receptor regions are represented by circles. Confirmed photolabeled receptor regions are represented by black circles. The calculated molecular masses of the photolabeled regions are shown and include the molecular mass of the photolabeled radioligand. Note that Asn residue glycosylation leads to an increase in apparent molecular mass of both the Ile2$^{(1.06)}$-Met30$^{(1.34)}$ (20.5-100 kDa) and Leu143$^{(4.40)}$-Met243$^{(6.38)}$ (100 kDa) receptor regions.

The analogues **B1**, **T1**, **B2**, and **T2** presented reduced binding affinities for the WT receptor, but were full agonists. Analogues **B3** and **T3** exhibited affinities that were similar to that of the native AngII peptide for the WT receptor, but both had partial agonistic properties. However, analogues **B1**, **T1**, **B2**, **T2**, **B3**, and **T3** not only displayed AngII-like binding affinities for CAM receptor, but were also complete agonists. Despite being referred to as significant pharmacophores,[17−20,30] Asp1 and Arg2 were unexpectedly and totally amenable to Bpa and Tdf photoprobe substitutions in the CAM receptor. However, both the WT and CAM receptors maintained a much more stringent SAR for the other amino acid positions of the AngII peptide. Analogues **B4** and **T4** exhibited prohibitively low affinities for both receptors. This aromatic amino acid is known to be of primordial importance in the interaction of the AngII ligand with its cognate receptor.[21,22,33−36] In contrast, the analogues **B5** and **T5** confirmed once again the total SAR permissiveness of the CAM receptor with AngII-like binding affinities and a full agonist profile, while these analogues exhibited extremely low affinity for the WT receptor. Analogues **B6**, **T6**, **B7**, and **T7** displayed

prohibitively low binding affinities for the WT-hAT$_1$ receptor but only reduced affinities for the CAM-hAT$_1$ receptor, in accordance with the biological significance of the imidazole ring of His6 and pyrrolidine ring of Pro7.[17−20] **B8** and **T8** were the analogues with the most conservative substitutions and confirmed AngII-like binding affinities for both the WT and CAM receptors, but with neutral antagonist and weak partial agonist characteristics on both receptors, respectively. An increase in the steric hindrance of the aromatic ring of the Phe8 amino acid has been shown to confers antagonistic properties on such AngII analogues.[37]

Despite the fact that the CAM receptor has a more tolerant SAR than the WT receptor, their ligand/receptor interactions appear to be equivalent. An exhaustive mutagenesis and photoaffinity labeling study using the analogue ^{125}I-**B8** on both receptors showed that they have comparable liganded receptor structures.[38] Since the CAM receptor retained nearly native pharmacological properties (i.e., in regard to the respective K_i as well as IP_1 production levels) for the analogues **B1**, **T1**, **B2**, **T2**, **B3**, **T3**, **B5**, and **T5**, the active-state receptor binding cleft probed by theses analogues should also be similar to that of the liganded WT receptor. To follow the ligand/receptor contact along the AngII ligand sequence, the CAM receptor was thus the only viable strategy and should provide valuable information on the AngII/AT$_1$ interaction.

The second aim of the present study was to elucidate the different regions of the hAT$_1$ receptor binding cleft that interact with a given position of the AngII ligand. Our previous studies showed that amino acid positions 1 and 3 of the AngII ligand interact with ECL 2 of the hAT$_1$ receptor and, in particular, position 3 interacts with residue Ile172$^{(4.69)}$.[12,13] The AngII carboxyl-terminus Phe8 interacts deeper within the space created by the TMD core of the hAT$_1$ receptor at residues Phe77$^{(2.53)}$ in TMD 2; Leu112$^{(3.36)}$ and Tyr113$^{(3.37)}$ in TMD 3; Asn200$^{(5.43)}$ in TMD 5; Phe249$^{(6.44)}$, Trp253$^{(6.48)}$, His256$^{(6.51)}$, and Thr260$^{(6.55)}$ in TMD 6; and Phe293$^{(7.44)}$, Asn294$^{(7.45)}$ Asn295$^{(7.46)}$, Cys296$^{(7.47)}$, and Leu297$^{(7.48)}$ in TMD 7.[14−16] The integration of these experimentally determined ligand/receptor contacts in in silico molecular modeling of GPCR X-ray crystal structures resulted in an evidence-based homology model of the AngII-liganded hAT$_1$ receptor complex where the interaction of the AngII carboxyl-terminus with the hAT$_1$ receptor is practically identical to that of the retinal/bovine rhodopsin complex.[16] Nevertheless, the individual interaction of the AngII amino acids positions 2, 4, 5, 6, and 7 with the various domains of the hAT$_1$ receptor remain unresolved.

The results presented herein (Figures 2−4 and Scheme 1) show that the AngII amino-terminus simultaneously contacts several regions of the hAT$_1$ receptor, including ectodomains such as NT and ECL 1. However, we could not totally exclude the interaction of the AngII amino-terminus with both the ECL 2 and ECL 3 of the hAT$_1$ receptor. The NT of the AT$_1$ receptor is known to contain essential AngII ligand-binding epitopes, in particular adjacent to the top of TMD 1.[39,40] The ECL 1 of the AT$_1$ receptor possesses a W94$^{(2.70)}$X95$^{(2.71)}$-F96$^{(2.72)}$G97$^{(2.73)}$ conserved motif, which has previously been postulated to form a type II β-turn and to be involved in AngII binding.[41,42] This motif has also been shown to be important for ligand-mediated activation in another rhodopsin-like GPCR, namely, the complement component 5a receptor.[43] In addition, various reports have provided evidence supporting the essential role of these extracellular regions in AngII ligand binding and hAT$_1$ receptor functions.[44−50]

We also took advantage of the complementary photochemical properties of both the Bpa and Tdf photoprobes to obtain further direct biochemical evidence of the AngII ligand-binding environment. The photogenerated biradical ketone intermediate of Bpa displays extremely low reactivity with water. On the other hand, the electrophilic nature of the much more reactive photogenerated carbene intermediate of Tdf causes this photoprobe to also react with water molecules and, thus, competes for and may even prevent receptor photolabeling.[23,51−54] A significant reduction in the respective photoaffinity labeling yields (Table 3) of the ^{125}I-Tdf-substituted AngII analogues compared to the ^{125}I-Bpa-substituted AngII analogues may provide an indication of the presence or absence of water molecules in or close to the ligand-binding environment of the hAT$_1$ receptor structure.

For analogues substituted at positions 1 and 2, the Tdf photolabeling yields were respectively 5.4- and 4.0-fold lower than those of the corresponding Bpa analogue, suggesting the presence of water molecules in the vicinity of the amino-terminus of the AngII ligand. In fact, analogues substituted by the water-sensitive Tdf photoprobe exhibited the lowest yields. Analogues ^{125}I-**B1** and ^{125}I-**T2** photolabeled the hydrophilic Asn4$^{(1.08)}$-Asn25$^{(1.29)}$ region of the NT of the hAT$_1$ receptor, among other regions. For GPCRs activated by diffusible ligands like the beta-2 adrenergic receptor, the water-accessible NT is disordered and has no clear contacts with either the ECLs or TMDs.[55] In contrast, analogues substituted at positions 3, 5, and 8, which are reputed to interact more deeply within the TMDs core of the receptor, did not display any significant differences in Bpa and Tdf photolabeling yields, suggesting that there is a hydrophobic, water-free environment in the vicinity of the center and carboxyl-terminus of the AngII ligand. A single large region, Leu143$^{(4.40)}$-Met243$^{(6.38)}$, spanning from TDM4 through ECL 3 of the hAT$_1$ receptor was photolabeled both by analogues ^{125}I-**B3** and ^{125}I-**T3**. This receptor region encompasses the AngII contact at position Ile172$^{(4.69)}$ in ECL 2.[13] Crystallography and nuclear magnetic resonance spectroscopy experiments on opsin[56] and rhodopsin[57,58] confirmed that the ECL 2 folds back deeply into the hydrophobic center of the receptor protein and contributes to the retinal-binding site as a "retinal plug". In addition, substituted-cysteine scanning mutagenesis[59,60] and crystallographic studies[61,62] on rhodopsin-like aminergic GPCRs also indicated that the ECL 2 contacts the ligand in the binding cleft of the receptor. Analogues ^{125}I-**B5** and ^{125}I-**T5** photolabeled both the NT and the ECL 1 of the hAT$_1$ receptor, presumably close to or at the extracellular region/TMDs interface. Various residues located deeper within the TMDs hydrophobic core of the hAT$_1$ receptor are photolabeled by analogue ^{125}I-**B8**,[12,14−16] while analogue ^{125}I-**T8** simultaneously photolabels receptor residues on TMDs 3 and 6.[63,64] Unfortunately, no photoaffinity labeling experiments were performed with analogues substituted at positions 4, 6, and 7, since their binding affinities and/or photolabeling yields prevented further investigation.

Conclusion

In light of results provided in the present study, the CAM-hAT$_1$ receptor has a SAR more amenable to amino acid substitution at positions 1, 2, 3, and 5 of the AngII octapeptide sequence than that of the WT receptor. Photoaffinity labeling has been previously used to gain information on the WT

receptor binding environment of positions 1 and 3 of AngII. Now, analogues containing photoprobe amino acids in positions 2 and 5 are available to further characterize the AT_1 receptor binding cleft, using the CAM receptor. The use of both the Bpa and Tdf photoprobe amino acids, which exhibit different but complementary photochemical properties, evidenced that the AngII amino-terminus resides in a hydrophilic environment and interacts simultaneously with several regions of the CAM-hAT_1 receptor, including ectodomains such as the NT and ECL 1. Nevertheless, the interaction of both the ECL 2 and ECL 3 of the CAM-hAT_1 receptor with the AngII amino-terminus could not be totally excluded. Altogether, these results should be valuable in order to guide an in-depth and more exhaustive investigation aimed at identifying the precise receptor residues that contact AngII using the methionine proximity assay.[14,16,38,65]

Experimental Section

Materials. Starting materials and reagents for the peptide syntheses were from Novabiochem (San Diego, CA, USA). The *p*-benzoyl-L-phenylalanine photoprobe amino acid was from Chem-Impex International Inc. (Wood Dale, IL, USA), whereas the *p*-[3-(trifluoromethyl)-3*H*-diazirin-3-yl]-L-phenylalanine (Tdf) photoprobe amino acid was previously synthesized by us.[23] Pyrex tubes, solvents, and all inorganic chemicals were from Fisher Scientific (Pittsburgh, PA, USA). All organic chemicals were from Sigma-Aldrich (St. Louis, MO, USA). IODO-GEN iodination reagent (1,3,4,6-tetrachloro-3*R*,6*R*-diphenylglycoluril) was from Pierce Protein Research Products (Rockford, IL, USA). $Na^{125}I$ was from Perkin-Elmer Inc. (Wellesley, MA, USA). The plasmid containing the human AT_1 receptor subcloned in the mammalian expression vector pcDNA3.0 was kindly provided by Dr. Sylvain Meloche (Université de Montréal, Montreal, QC, Canada). Site-directed mutagenesis materials (QuikChange II XL Site-Directed Mutagenesis Kit) were from Stratagene (La Jolla, CA, USA). Cell culture materials, the pcDNA3.0 plasmid, oligonucleotides, and low molecular mass protein standards were from Gibco (Invitrogen, Carlsbad, CA, USA). FuGENE 6 transfection reagent, Complete Protease Inhibitor Cocktail, Nonidet P-40, endoproteinase Lys-C sequencing grade (endoLys-C, EC 3.4.21.50), and peptide-*N*-glycosidase F peptide-N^4-(acetyl-β-glucosaminyl)-asparagine amidase (PNGase F; EC 3.5.1.52) were from Roche Applied Science (Indianapolis, IN, USA). Bovine serum albumin (BSA) and bacitracin were from Sigma-Aldrich. Binding filters (1.0 μm grade GF/B glass microfiber, Whatman) were from VWR International (Arlington Heights, IL, USA). Inositol-1-monophosphate production assays (IP-One HTRF Assay) were from Cisbio (Bedford, MA, USA). Flat-bottom white 96-well assay microplates were from Corning (Corning, NY, USA). Mini-spiral black light self-ballasted ultraviolet lamps (13 W, 120 V, 60 Hz, 225 mA, λ_{max} 365 nm) were from Noma (Toronto, ON, Canada). Amicon Ultra-15 centrifugal filter devices with a 10 000 MWCO were from Millipore (Billerica, MA, USA). Electrophoresis materials and Precision Plus Protein Prestained Standards were from Bio-Rad Laboratories (Hercules, CA, USA). Gel drying kits with permeable cellophane films were from Promega Corporation (Madison, WI, USA). BioMax MR X-ray intensifying films were from Kodak (Rochester, NY, USA).

Numbering of GPCRs. The residues of the hAT_1 receptor were given two numbering schemes. First, residues were numbered based on their positions in the hAT_1 receptor sequence. Second, represented in superscript within parentheses, residues were numbered on the basis of their position relative to the most conserved residue in their respective TMDs within rhodopsin-like GPCRs accordingly to Ballesteros and Weinstein.[66] This indexing simplifies the identification of aligned residues in different GPCRs. By definition, the most conserved residue was assigned the position index 50, with incremental numbering of downstream residues and decremental numbering of upstream residues. The indexed residues are $Asn46^{(1.50)}$, $Asp74^{(2.50)}$, $Arg126^{(3.50)}$, $Trp153^{(4.50)}$, $Pro207^{(5.50)}$, $Pro255^{(6.50)}$, and $Pro299^{(7.50)}$.

Peptide Synthesis and Radiolabeling. *p*-Benzoyl-L-phenylalanine (Bpa) and *p*-[3-(trifluoromethyl)-3*H*-diazirin-3-yl]-L-phenylalanine (Tdf) photoprobe amino acids substituted AngII peptide analogues were synthesized using the standard solid-phase peptide synthesis method with *N*-[(9-fluorenyl)-methoxycarbonyl] (Fmoc)-protected amino acids and Wang resin (*p*-benzyloxybenzyl alcohol resin) as previously reported.[24,26] Once the synthesis was completed, the side chain protecting group and resin linker were simultaneously cleaved. The crude peptides were purified by reversed-phase high-pressure liquid chromatography (RP-HPLC) on a Waters 625 LC instrument equipped with a Waters C-18 reversed-phase column and monitored by absorbance at 214 nm as well as by γ-counting when necessary. Peptides were eluted as a single signal and were at least 95% pure. The mass spectrum of each peptide analogue was obtained using a Tofspec2 Micromass instrument with matrix-assisted laser desorption ionization time-of-flight (MALDI-TOF; see Supporting Information). The resulting peptides were then radiolabeled using the IODO-GEN iodination method as described by Fraker and Speck.[67] In brief, in the following order, 500 mM potassium phosphate buffer (K_2HPO_4/KH_2PO_4, pH 5.0, 30 μL), 1 mM AngII analogue (10 μL, 1.0 mol equiv), and 45 μM (5 mCi) $Na^{125}I$ (10 μL, 1 mCi, 0.045 mol equiv) were added to a 250 μL Eppendorf tube coated with IODO-GEN (20.0 μg, 4.6 mol equiv) in a final volume of 50 μL. The solutions were incubated at room temperature for 15−20 min in the dark. The reaction conditions were optimized to form monoiodinated peptide analogues. The reaction mixtures were stopped by adding 50 μL of quenching solution (0.2 mM Na_2SO_3, 0.2 mM KI, pH 7) and incubated at room temperature for an additional 15 min in the dark. The radiolabeled peptides were purified by RP-HPLC with a 20−40% acetonitrile gradient containing 0.05% aqueous α,α,α-trifluoroacetic acid. Typical retention times were 14−18 min for the 29−33% acetonitrile portion of the gradient. The specific radioactivity of the radiolabeled peptides was 1500 ± 500 Ci/mmol as determined by homologous competition binding affinity assays as reported by Wiener and Reith.[68,69] Stock solutions of radiolabeled peptide analogues were adjusted to pH 7.0, diluted in BSA (1 μM final concentration), flash−frozen in liquid nitrogen, and stored at −80 °C until used. Under these conditions, we typically obtained yields of 15−70% pure ^{125}I-radiolabeled photoreactive AngII peptide analogues as a white amorphous solid. Note that the photoreactive Tdf-containing peptide analogues were handled in amber flasks in dim light.

Site-Directed Mutagenesis. Oligonucleotide site-directed mutagenesis was performed using QuikChange II XL site-directed mutagenesis kits as described by Stratagene. Constitutively active mutant [N111G]-hAT_1 receptor cDNA was generated using WT-hAT_1 receptor cDNA subcloned into the *Hin*dIII-XbaI sites of the mammalian expression vector pcDNA3.0 as a template. Sets of forward and reverse oligonucleotides were constructed and used to introduce a single Asn-Gly mutation at position $111^{(3.35)}$ of the hAT_1 receptor. Site-directed mutations were then confirmed by automated DNA sequencing by aligning the hAT_1 receptor sequence using *Sequencher 4.9* software (Gene Codes Corporation, Ann Arbor, MI, USA).

Cell Culture and Transfections. COS-7 cells were grown in Dulbecco's Modified Eagle's Medium (DMEM) supplemented with 2 mM L-glutamine, 10% [v/v] fetal bovine serum (FBS), 100 IU/mL penicillin, and 100 μg/mL of streptomycin. The cells were seeded into 100 mm diameter cell culture dishes in 10 mL of the same medium and incubated at 37 °C in a 5% [v/v] CO_2 atmosphere until the density reached (6−8) × 10^6 cells/dish.

Following a trypsin treatment, 1.5×10^6 cells were suspended in 10 mL of the same medium and grown in 100-mm-diameter cell culture dishes for 24 h. Transfections were performed using FuGENE 6 transfection reagent as described by Roche Applied Science. Briefly, serum-free DMEM (172 μL) was incubated with FuGENE 6 transfection reagent (18 μL) at room temperature for 5 min. Plasmid DNA (6 μg, 60 μL) was then added and the solution (250 μL final volume) was incubated at room temperature for 30 min. The cells were transiently transfected by adding the transfection solutions (250 μL/dish). Transfected cells were grown for an additional 36 h at 37 °C in a 5% [v/v] CO_2 atmosphere. The cells were washed once with phosphate-buffered saline (PBS; 137 mM NaCl, 0.9 mM $MgCl_2$, 3.5 mM KCl, 0.9 mM $CaCl_2$, 8.7 mM Na_2HPO_4, and 3.5 mM NaH_2PO_4), immediately flash-frozen in liquid nitrogen, and stored at −80 °C until used. Frozen cells were subjected to one freeze−thaw cycle (1 min at 37 °C), and 10 mL of ice-cold washing buffer (5 mM $MgCl_2$, 25 mM Trizma-Base, 100 mM NaCl; pH 7.4) was added to the broken cells. The cells were then gently scraped from the bottom of the wells and were transferred into a 15 mL centrifuge tube. The cell membrane suspensions were centrifuged (500 *g* for 15 min at 4 °C) and the supernatants were removed. The transfected COS-7 cell pellets were immediately stored at −80 °C until used.

Competition Binding Affinity Assay. The cell pellets were resuspended in 10 mL of ice-cold binding buffer (5 mM $MgCl_2$, 25 mM Trizma-Base, 100 mM NaCl, 0.1% [w/v] bovine serum albumin (BSA), and 0.01% [w/v] bacitracin, pH 7.4). For the heterologous competition binding assay, 30 aliquots of the resulting cell membrane suspensions (50−100 μg total protein) were independently incubated until complete equilibrium (room temperature for 1 h in the dark in a final volume of 500 μL of binding buffer) with increasing concentrations (15 different concentrations in duplicate from 10 μM to 1 ρM with half-log increases) of AngII analogues and 0.1 nM of ^{125}I-[Sar_1, Ile_8]AngII (^{125}I-Sarile; 1500 ± 500 Ci/mmol) as a radioactive tracer. Total binding was measured in the presence of 1 pM unlabeled ligand and 0.1 nM ^{125}I-[Sar_1,Ile_8]AngII (^{125}I-Sarile; 1500 ± 500 Ci/mmol), whereas nonspecific binding was measured in the presence of 10 μM unlabeled ligand and 0.1 nM ^{125}I-[Sar_1,Ile_8]AngII (^{125}I-Sarile; 1500 ± 500 Ci/mmol). Bound radioligand was separated from free radioligand by vacuum filtration at 4 °C through filters presoaked in binding buffer (at room temperature for 1 h). Receptor-bound radioligand was evaluated by γ-counting. Under these experimental conditions, total binding was typically 2500 ± 1000 cpm while nonspecific binding was typically 500 ± 250 cpm. Binding data were analyzed with a nonlinear regression curve-fitting routine performed using GraphPad *Prism v 5.00* for Windows (GraphPad Software, San Diego, CA, USA).

Ligand-Induced Inositol-1-Monophosphates Production Assay. COS-7 cells were grown in Dulbecco's Modified Eagle's Medium (DMEM) supplemented with 2 mM L-glutamine, 10% [v/v] fetal bovine serum (FBS), 100 IU/mL of penicillin, and 100 μg/mL of streptomycin. The cells were seeded into 96-well cell culture plates (5000 cells/well) in 100 μL of the same medium and incubated at 37 °C in a 5% [v/v] CO_2 atmosphere for 24 h. Transfections were performed using FuGENE 6 transfection reagent as described by Roche Applied Science. Briefly, serum-free DMEM (87 μL) was incubated with FuGENE 6 transfection reagent (3 μL) at room temperature for 5 min. Plasmid DNA (1 μg in 10 μL) was then added and the solution (100 μL final volume) was incubated at room temperature for 30 min. The cells were transiently transfected by adding the transfection solution (5 μL/well). Transfected cells were grown for an additional 24 h at 37 °C in a 5% [v/v] CO_2 atmosphere. The inositol-1-monophosphate (IP_1) production assay was performed using IP-One HTRF assay (Terbium) kits as described by Cisbio. Briefly, basal (vehicle) and stimulated (1×10^{-6} M final concentration of AngII analogue) IP_1 production were induced for 30 min at 37 °C in a 5% [v/v] CO_2 atmosphere in triplicate, and parallel wells were used to measure receptor expression. IP_1 levels were adjusted on the basis of receptor expression levels. Samples were transferred from the 96-well cell culture plates to flat bottom white 96-well assay microplates, and FRET fluorescence readouts were performed with a Tecan Infinite M1000 premium Quad4 Monochromator.

Photoaffinity Labeling Experiments. The cell pellets were resuspended in 500 μL of binding buffer at 37 °C (5 mM $MgCl_2$, 25 mM Trizma-Base, 100 mM NaCl, 0.1% [w/v] bovine serum albumin (BSA), and 0.01% [w/v] bacitracin, pH 7.4). For the photoaffinity labeling experiments, the resulting cell membrane suspensions (50−100 μg of total protein) were incubated at 37 °C for 1 h in the dark in a final volume of 500 μL of binding buffer with 10−25 nM of radiolabeled photoreactive AngII analogue (1500 ± 500 Ci/mmol). The cell membranes were then centrifuged at 500 *g* for 15 min at 4 °C. The cell pellets were resuspended in 500 μL of 37 °C washing buffer (5 mM $MgCl_2$, 25 mM Trizma-Base, 100 mM NaCl, pH 7.4) and irradiated ($h\nu$ = 350−360 nm) at 37 °C for 1 h in a temperature-controlled photoreaction chamber (±1 °C) in a 5 mL Pyrex tube immersed in distilled water within the spiral cage of the ultraviolet lamp. The cell membranes were centrifuged at 2500*g* for 15 min at 4 °C. The cell pellets were solubilized in modified radio-immunoprecipitation buffer (mRIPA; 0.1% [w/v] SDS (electrophoresis grade), 0.25% [w/v] sodium deoxycholate, 1% [v/v] Nonidet P-40, 5 mM NaN_3, 50 mM Trizma-HCl (pH 7.4), and 150 mM NaCl) supplemented with Complete Protease Inhibitor Cocktail and incubated on ice for 1 h. The cell lysates were centrifuged at 2500 *g* for 30 min at 4 °C to remove insoluble materials. The supernatant containing the solubilized photolabeled ligand/receptor complexes was flash-frozen in liquid nitrogen and stored at −80 °C until they were partially purified.

Partial Purification of the Photolabeled Ligand/Receptor Complexes. The solubilized ligand/receptor photolabeled complexes were diluted with Laemmli loading buffer (0.1% [w/v] bromophenol blue, 2% [w/v] SDS, 10% [v/v] glycerol, 50 mM Trizma-HCl (pH 6.8), and 1% [v/v] β-mercaptoethanol) and incubated at 37 °C for 1 h. Sodium dodecyl sulfate polyacrylamide gel electrophoresis (SDS-PAGE) with tris-glycine buffer was performed essentially as described elsewhere[70] using 8% preparative gels. To locate the photolabeled ligand/receptor complexes, the gels were exposed to an X-ray film with an intensifying screen. Precision Plus Protein Prestained Standards were used to determine the apparent molecular masses. Radioactive bands were excised from the gel and the radioactive content was measured by γ-counting to assess recovery yield. The photolabeled ligand/receptor complexes were than passively eluted from the gel slices by maceration in 15 mL of tris-glycine electrophoresis buffer (250 mM glycine, 25 mM Trizma base, 0.1% [w/v] SDS) at 4 °C for 3 days with gentle agitation. The macerated gel slices were centrifuged at 2500 *g* for 15 min at 4 °C, and the supernatants containing the eluted photolabeled ligand/receptor complexes were concentrated to a final volume of 100−250 μL using Amicon Ultra-15 centrifugal filter devices (10 000 MWCO) as described by Millipore. The partially purified photolabeled ligand/receptor complexes were flash-frozen in liquid nitrogen and stored at −80 °C until use. Under these conditions, we typically recovered at least 70% of the initial radioactivity.

Photoaffinity Labeling Yields of Covalent Incorporation. The yields of covalent incorporation of the selected radiolabeled photoreactive AngII analogues were calculated as follows: [CPM count of photolabeled ligand/receptor complex from the SDS-PAGE of the partial purification step] ÷ [CPM count of related specific binding] × 100%. The same cell membrane preparations as well as the same radioligand were used in both the numerator and denominator for the calculation.

CNBr Cleavages of Met. The reactions were performed with 0.47 M CNBr in 70% [v/v] formic acid/10% [v/v] acetonitrile.

Partially purified photolabeled ligand/receptor complexes (0.1−1 ng containing 3−15 nCi) were lyophilized for 24 h. The lyophilized samples were then dissolved in a mixture of 90 μL of 77.7% [v/v] formic acid and 10 μL of CNBr (5 mg) dissolved in acetonitrile for a total volume of 100 μL. The solutions were then incubated at room temperature for 18 h in the dark. The reaction mixtures were quenched by adding 1 mL of water and were lyophilized for 24 h. The samples were flash-frozen in liquid nitrogen and stored at −80 °C until analyzed. Note that CNBr is particularly toxic and was handled in a fume hood. The reactions were performed in sealed polypropylene ware.

Peptide-*N*-glycosidase F Peptide-N^4-(acetyl-β-glucosaminyl)-asparagine Amidase (PNGase F) Deglycosylations. Prior to performing the PNGase F deglycosylations, the CNBr-treated lyophilized samples were partially purified as previously reported (see Partial Purification of the Photolabeled Ligand/Receptor Complexes) using an SDS-PAGE procedure as described below (see Analysis of the Proteolysis Products). The radioactive glycoprotein bands with apparent molecular masses greater than 12.5 kDa were the only ones that passively eluted. They were lyophilized for 24 h and were deglycosylated using PNGase F. The lyophilized samples were dissolved in 100 μL of digestion buffer (50 mM Tris-Base, 25 mM EDTA, 0.5% [v/v] Nonidet NP-40, 0.1% [w/v] SDS, 1% [v/v] β-mercaptoethanol, pH 8.0) containing 10 U of PNGase F. The solutions were incubated at room temperature for 16 h in the dark. The reaction mixtures were quenched by adding 1 mL of water and were lyophilized for 24 h. The samples were flash-frozen in liquid nitrogen and stored at −80 °C until analysis.

Endoproteinase Lys-C (EndoLys-C) Digestions. Partially purified photolabeled ligand/receptor complexes (0.1−1 ng containing 3−15 nCi) were lyophilized for 24 h. The lyophilized samples were dissolved in 100 μL of digestion buffer (25 mM Tris-Base, 1 mM EDTA, 0.1% [w/v] SDS, pH 8.5) containing 1 μg of endoLys-C. The solutions were incubated at 37 °C for 16 h in the dark. The reaction mixtures were quenched by adding 1 mL of water and were lyophilized for 24 h. The samples were flash-frozen in liquid nitrogen and stored at −80 °C until analysis.

Analysis of the Proteolysis Products. The proteolysis products generated from the chemical cleavage and enzymatic digestion of the photolabeled ligand/receptor complexes were analyzed by analytical sodium dodecyl sulfate polyacrylamide gel electrophoresis (SDS-PAGE) with Tris-tricine buffer. The procedures were performed essentially as reported by Schagger and von Jagow.[71,72] For routine analyses (as for Figure 4), 4% T/3% C stacking gels and 16.5% T/4.5% C separating gels with glycerol were used. For more precise analyses (as for glycoprotein bands in Figure 3), 2-cm-long 4% T/3% C stacking gels, 3-cm-long 10% T/3% C spacer gels, and 13-cm-long 16.5% T/4.5% C separating gels with glycerol were run at room temperature for 24−36 h. Low molecular mass protein standards were used to determine apparent molecular masses. The gels were fixed in gel fixation buffer (7.5% [v/v] glacial acetic acid, 10% [v/v] glycerol, 40% [v/v] methanol) at room temperature for 5−10 min. The gels were dried as described elsewhere[70] or with permeable cellophane film gel drying kits as described by Promega Corporation. Radioactive bands were revealed using X-ray intensifying films. Typical exposure times were 3−4 days for an initial γ-count of 3 nCi and 12−24 h for an initial γ-count of 15 nCi.

Acknowledgment. The authors thank Marie-Reine Lefebvre (Université de Sherbrooke, Sherbrooke, QC, Canada) for her expert help and technical assistance, Dr. Brian J. Holleran (Université de Sherbrooke, Sherbrooke, QC, Canada) for his critical reading of the manuscript, Dr. Richard Leduc (Université de Sherbrooke, Sherbrooke, QC, Canada), and Dr. Jean-Bernard Denault (Université de Sherbrooke, Sherbrooke, QC, Canada) for providing access to his facilities as well as Dr. Sylvain Meloche (Université de Montréal, Montreal, QC, Canada) for the human AT_1 receptor clone. This work was supported by the Canadian Institutes of Health Research. E.E. is a recipient of the J.C. Edwards Chair in Cardiovascular Research. This article was submitted to fulfill the requirements of a Ph.D. thesis for D.F. at the Université de Sherbrooke.

Supporting Information Available: MALDI-TOF HRMS data for all synthesized photoreactive AngII analogues, **B1** to **B8** and **T1** to **T8**. This material is available free of charge via the Internet at http://pubs.acs.org.

References

(1) Pierce, K. L.; Premont, R. T.; Lefkowitz, R. J. Seven-transmembrane receptors. *Nat. Rev. Mol. Cell Biol.* **2002**, *3*, 639–650.
(2) Bockaert, J.; Pin, J. P. Molecular tinkering of G protein-coupled receptors: an evolutionary success. *Embo J.* **1999**, *18*, 1723–1729.
(3) Fredriksson, R.; Lagerstrom, M. C.; Lundin, L. G.; Schioth, H. B. The G-protein-coupled receptors in the human genome form five main families. Phylogenetic analysis, paralogon groups, and fingerprints. *Mol. Pharmacol.* **2003**, *63*, 1256–1272.
(4) Kobilka, B. K. G protein coupled receptor structure and activation. *Biochim. Biophys. Acta* **2007**, *1768*, 794–807.
(5) Gether, U. Uncovering molecular mechanisms involved in activation of G protein-coupled receptors. *Endocr. Rev.* **2000**, *21*, 90–113.
(6) Ji, T. H.; Grossmann, M.; Ji, I. G protein-coupled receptors. I. Diversity of receptor-ligand interactions. *J. Biol. Chem.* **1998**, *273*, 17299–17302.
(7) Vodovozova, E. L. Photoaffinity labeling and its application in structural biology. *Biochemistry* (*Mosc.*) **2007**, *72*, 1–20.
(8) Hatanaka, Y.; Sadakane, Y. Photoaffinity labeling in drug discovery and developments: chemical gateway for entering proteomic frontier. *Curr. Top. Med. Chem.* **2002**, *2*, 271–288.
(9) Dorman, G.; Prestwich, G. D. Using photolabile ligands in drug discovery and development. *Trends Biotechnol.* **2000**, *18*, 64–77.
(10) Dorman, G. Photoaffinity labeling in biological signal transduction. *Top. Curr. Chem.* **2000**, *211*, 169–225.
(11) de Gasparo, M.; Catt, K. J.; Inagami, T.; Wright, J. W.; Unger, T. International union of pharmacology. XXIII. The angiotensin II receptors. *Pharmacol. Rev.* **2000**, *52*, 415–472.
(12) Laporte, S. A.; Boucard, A. A.; Servant, G.; Guillemette, G.; Leduc, R.; Escher, E. Determination of peptide contact points in the human angiotensin II type I receptor (AT1) with photosensitive analogs of angiotensin II. *Mol. Endocrinol.* **1999**, *13*, 578–586.
(13) Boucard, A. A.; Wilkes, B. C.; Laporte, S. A.; Escher, E.; Guillemette, G.; Leduc, R. Photolabeling identifies position 172 of the human AT(1) receptor as a ligand contact point: receptor-bound angiotensin II adopts an extended structure. *Biochemistry* **2000**, *39*, 9662–9670.
(14) Clement, M.; Martin, S. S.; Beaulieu, M. E.; Chamberland, C.; Lavigne, P.; Leduc, R.; Guillemette, G.; Escher, E. Determining the environment of the ligand binding pocket of the human angiotensin II type I (hAT1) receptor using the methionine proximity assay. *J. Biol. Chem.* **2005**, *280*, 27121–27129.
(15) Perodin, J.; Deraet, M.; Auger-Messier, M.; Boucard, A. A.; Rihakova, L.; Beaulieu, M. E.; Lavigne, P.; Parent, J. L.; Guillemette, G.; Leduc, R.; Escher, E. Residues 293 and 294 are ligand contact points of the human angiotensin type 1 receptor. *Biochemistry* **2002**, *41*, 14348–14356.
(16) Clement, M.; Cabana, J.; Holleran, B. J.; Leduc, R.; Guillemette, G.; Lavigne, P.; Escher, E. Activation induces structural changes in the liganded angiotensin II type 1 receptor. *J. Biol. Chem.* **2009**, *284*, 26603–26612.
(17) Tzakos, A. G.; Gerothanassis, I. P.; Troganis, A. N. On the structural basis of the hypertensive properties of angiotensin II: a solved mystery or a controversial issue? *Curr. Top. Med. Chem.* **2004**, *4*, 431–444.
(18) Peach, M. J. Structural features of angiotensin II which are important for biologic activity. *Kidney Int. Suppl.* **1979**, S3–6.
(19) Regoli, D.; Park, W. K.; Rioux, F. Pharmacology of angiotensin. *Pharmacol. Rev.* **1974**, *26*, 69–123.
(20) Khosla, M.; Smeby, R.; Bumpus, F. Structure activity relationship in angiotensin II analogs, In *Handbook of Experimental Pharmacology*; Springer: New York-Heidelberg-Berlin, 1974; Vol XXXVII, pp 126−156.
(21) Feng, Y. H.; Miura, S.; Husain, A.; Karnik, S. S. Mechanism of constitutive activation of the AT1 receptor: influence of the size of

the agonist switch binding residue Asn(111). *Biochemistry* **1998**, *37*, 15791–15798.
(22) Noda, K.; Feng, Y. H.; Liu, X. P.; Saad, Y.; Husain, A.; Karnik, S. S. The active state of the AT1 angiotensin receptor is generated by angiotensin II induction. *Biochemistry* **1996**, *35*, 16435–16442.
(23) Fillion, D.; Deraet, M.; Holleran, B. J.; Escher, E. Stereospecific synthesis of a carbene-generating angiotensin II analogue for comparative photoaffinity labeling: improved incorporation and absence of methionine selectivity. *J. Med. Chem.* **2006**, *49*, 2200–2209.
(24) Bosse, R.; Servant, G.; Zhou, L. M.; Boulay, G.; Guillemette, G.; Escher, E. Sar1-p-benzoylphenylalanine-angiotensin, a new photoaffinity probe for selective labeling of the type 2 angiotensin receptor. *Regul. Pept.* **1993**, *44*, 215–223.
(25) Lanctot, P. M.; Leclerc, P. C.; Clement, M.; Auger-Messier, M.; Escher, E.; Leduc, R.; Guillemette, G. Importance of N-glycosylation positioning for cell-surface expression, targeting, affinity and quality control of the human AT1 receptor. *Biochem. J.* **2005**, *390*, 367–376.
(26) Laporte, S. A.; Servant, G.; Richard, D. E.; Escher, E.; Guillemette, G.; Leduc, R. The tyrosine within the NPXnY motif of the human angiotensin II type 1 receptor is involved in mediating signal transduction but is not essential for internalization. *Mol. Pharmacol.* **1996**, *49*, 89–95.
(27) Bayer, E. A.; Ben-Hur, H.; Wilchek, M. Analysis of proteins and glycoproteins on blots. *Methods Enzymol.* **1990**, *184*, 415–427.
(28) Durchschlag, H.; Christl, R.; Jaenicke, R. *Progress in Colloid and Polymer Science*; Springer: Berlin/Heidelberg, 1991; Vol 86, pp 41−56.
(29) Fyhrquist, F.; Saijonmaa, O. Renin-angiotensin system revisited. *J Intern. Med.* **2008**, *264*, 224–236.
(30) Pires, J. M.; Moore, G. J. Angiotensin charge relay system: role of arginine. *Proc. West Pharmacol. Soc.* **1998**, *41*, 197–199.
(31) Wilkes, B. C.; Masaro, L.; Schiller, P. W.; Carpenter, K. A. Angiotensin II vs its type I antagonists: conformational requirements for receptor binding assessed from NMR spectroscopic and receptor docking experiments. *J. Med. Chem.* **2002**, *45*, 4410–4418.
(32) Matsoukas, J. M.; Polevaya, L.; Ancans, J.; Mavromoustakos, T.; Kolocouris, A.; Roumelioti, P.; Vlahakos, D. V.; Yamdagni, R.; Wu, Q.; Moore, G. J. The design and synthesis of a potent Angiotensin II cyclic analogue confirms the ring cluster receptor conformation of the hormone Angiotensin II. *Bioorg. Med. Chem.* **2000**, *8*, 1–10.
(33) Miura, S.; Feng, Y. H.; Husain, A.; Karnik, S. S. Role of aromaticity of agonist switches of angiotensin II in the activation of the AT1 receptor. *J. Biol. Chem.* **1999**, *274*, 7103–7110.
(34) Tofovic, S. P.; Jackson, E. K. Tachyphylaxis to angiotensin II and [Phe4]-angiotensin II in the rat mesentery in vivo. *J. Pharmacol. Exp. Ther.* **1996**, *276*, 13–20.
(35) Moore, G. J.; Ganter, R. C.; Matsoukas, J. M.; Hondrelis, J.; Agelis, G.; Barlos, K.; Wilkinson, S.; Sandall, J.; Fowler, P. Receptor interactions of the position 4 side chains of angiotensin II analogues: importance of aromatic ring quadrupole. *J. Mol. Recognit.* **1994**, *7*, 251–256.
(36) Guillemette, G.; Bernier, M.; Parent, P.; Leduc, R.; Escher, E. Angiotensin II: dependence of hormone affinity on the electronegativity of a single side chain. *J. Med. Chem.* **1984**, *27*, 315–320.
(37) Aumelas, A.; Sakarellos, C.; Lintner, K.; Fermandjian, S.; Khosla, M. C.; Smeby, R. R.; Bumpus, F. M. Studies on angiotensin II and analogs: impact of substitution in position 8 on conformation and activity. *Proc. Natl. Acad. Sci. U.S.A.* **1985**, *82*, 1881–1885.
(38) Clement, M.; Chamberland, C.; Perodin, J.; Leduc, R.; Guillemette, G.; Escher, E. The active and the inactive form of the hAT1 receptor have an identical ligand-binding environment: an MPA study on a constitutively active angiotensin II receptor mutant. *J. Recept. Signal Transduct. Res.* **2006**, *26*, 417–433.
(39) Santos, E. L.; Pesquero, J. B.; Oliveira, L.; Paiva, A. C.; Costa-Neto, C. M. Mutagenesis of the AT1 receptor reveals different binding modes of angiotensin II and [Sar1]-angiotensin II. *Regul. Pept.* **2004**, *119*, 183–188.
(40) Hjorth, S. A.; Schambye, H. T.; Greenlee, W. J.; Schwartz, T. W. Identification of peptide binding residues in the extracellular domains of the AT1 receptor. *J. Biol. Chem.* **1994**, *269*, 30953–30959.
(41) Nicastro, G.; Peri, F.; Franzoni, L.; de Chiara, C.; Sartor, G.; Spisni, A. Conformational features of a synthetic model of the first extracellular loop of the angiotensin II AT1A receptor. *J. Pept. Sci.* **2003**, *9*, 229–243.
(42) Salinas, R. K.; Shida, C. S.; Pertinhez, T. A.; Spisni, A.; Nakaie, C. R.; Paiva, A. C.; Schreier, S. Trifluoroethanol and binding to model membranes stabilize a predicted turn in a peptide corresponding to the first extracellular loop of the angiotensin II AT(1A) receptor. *Biopolymers* **2002**, *65*, 21–31.
(43) Klco, J. M.; Nikiforovich, G. V.; Baranski, T. J. Genetic analysis of the first and third extracellular loops of the C5a receptor reveals an essential WXFG motif in the first loop. *J. Biol. Chem.* **2006**, *281*, 12010–12019.
(44) Baleanu-Gogonea, C.; Karnik, S. Model of the whole rat AT1 receptor and the ligand-binding site. *J. Mol. Model.* **2006**, *12*, 325–337.
(45) Hoe, K. L.; Saavedra, J. M. Site-directed mutagenesis of the gerbil and human angiotensin II AT(1) receptors identifies amino acid residues attributable to the binding affinity for the nonpeptidic antagonist losartan. *Mol. Pharmacol.* **2002**, *61*, 1404–1415.
(46) Correa, S. A.; Zalcberg, H.; Han, S. W.; Oliveira, L.; Costa-Neto, C. M.; Paiva, A. C.; Shimuta, S. I. Aliphatic amino acids in helix VI of the AT(1) receptor play a relevant role in agonist binding and activity. *Regul. Pept.* **2002**, *106*, 33–38.
(47) Correa, S. A.; Franca, L. P.; Costa-Neto, C. M.; Oliveira, L.; Paiva, A. C.; Shimuta, S. I. Relevant role of Leu265 in helix VI of the angiotensin AT1 receptor in agonist binding and activity. *Can. J. Physiol. Pharmacol.* **2002**, *80*, 426–430.
(48) Gosselin, M. J.; Leclerc, P. C.; Auger-Messier, M.; Guillemette, G.; Escher, E.; Leduc, R. Molecular cloning of a ferret angiotensin II AT(1) receptor reveals the importance of position 163 for Losartan binding. *Biochim. Biophys. Acta* **2000**, *1497*, 94–102.
(49) Costa-Neto, C. M.; Miyakawa, A. A.; Oliveira, L.; Hjorth, S. A.; Schwartz, T. W.; Paiva, A. C. Mutational analysis of the interaction of the N- and C-terminal ends of angiotensin II with the rat AT(1A) receptor. *Br. J. Pharmacol.* **2000**, *130*, 1263–1268.
(50) Inoue, Y.; Nakamura, N.; Inagami, T. A review of mutagenesis studies of angiotensin II type 1 receptor, the three-dimensional receptor model in search of the agonist and antagonist binding site and the hypothesis of a receptor activation mechanism. *J. Hypertens.* **1997**, *15*, 703–714.
(51) Tate, J. J.; Persinger, J.; Bartholomew, B. Survey of four different photoreactive moieties for DNA photoaffinity labeling of yeast RNA polymerase III transcription complexes. *Nucleic Acids Res.* **1998**, *26*, 1421–1426.
(52) Deseke, E.; Nakatami, Y.; Ourisson, G. Intrinsic reactivities of amino acids toward photoalkylation with benzophenone - a study preliminary to photolabelling of the transmembrane protein glycophorin A. *Eur. J. Org. Chem.* **1998**, 243–251.
(53) Weber, P. J.; Beck-Sickinger, A. G. Comparison of the photochemical behavior of four different photoactivatable probes. *J. Pept. Res.* **1997**, *49*, 375–383.
(54) Fleming, S. A. Chemical reagents in photoaffinity labeling. *Tetrahedron* **1995**, *51*, 12479–12520.
(55) Cherezov, V.; Rosenbaum, D. M.; Hanson, M. A.; Rasmussen, S. G.; Thian, F. S.; Kobilka, T. S.; Choi, H. J.; Kuhn, P.; Weis, W. I.; Kobilka, B. K.; Stevens, R. C. High-resolution crystal structure of an engineered human beta2-adrenergic G protein-coupled receptor. *Science* **2007**, *318*, 1258–1265.
(56) Park, J. H.; Scheerer, P.; Hofmann, K. P.; Choe, H. W.; Ernst, O. P. Crystal structure of the ligand-free G-protein-coupled receptor opsin. *Nature* **2008**, *454*, 183–187.
(57) Palczewski, K.; Kumasaka, T.; Hori, T.; Behnke, C. A.; Motoshima, H.; Fox, B. A.; Le Trong, I.; Teller, D. C.; Okada, T.; Stenkamp, R. E.; Yamamoto, M.; Miyano, M. Crystal structure of rhodopsin: A G protein-coupled receptor. *Science* **2000**, *289*, 739–745.
(58) Ahuja, S.; Hornak, V.; Yan, E. C.; Syrett, N.; Goncalves, J. A.; Hirshfeld, A.; Ziliox, M.; Sakmar, T. P.; Sheves, M.; Reeves, P. J.; Smith, S. O.; Eilers, M. Helix movement is coupled to displacement of the second extracellular loop in rhodopsin activation. *Nat. Struct. Mol. Biol.* **2009**, *16*, 168–175.
(59) Shi, L.; Javitch, J. A. The second extracellular loop of the dopamine D2 receptor lines the binding-site crevice. *Proc. Natl. Acad. Sci. U.S.A.* **2004**, *101*, 440–445.
(60) Shi, L.; Javitch, J. A. The binding site of aminergic G protein-coupled receptors: the transmembrane segments and second extracellular loop. *Annu. Rev. Pharmacol. Toxicol.* **2002**, *42*, 437–467.
(61) Warne, T.; Serrano-Vega, M. J.; Baker, J. G.; Moukhametzianov, R.; Edwards, P. C.; Henderson, R.; Leslie, A. G.; Tate, C. G.; Schertler, G. F. Structure of a beta1-adrenergic G-protein-coupled receptor. *Nature* **2008**, *454*, 486–491.
(62) Rasmussen, S. G.; Choi, H. J.; Rosenbaum, D. M.; Kobilka, T. S.; Thian, F. S.; Edwards, P. C.; Burghammer, M.; Ratnala, V. R.; Sanishvili, R.; Fischetti, R. F.; Schertler, G. F.; Weis, W. I.; Kobilka, B. K. Crystal structure of the human beta2 adrenergic G-protein-coupled receptor. *Nature* **2007**, *450*, 383–387.
(63) Fillion, D.; Guillemette, G.; Leduc, R.; Escher, E. In *Agonist Activation of the Angiotensin II Type 1 Receptor Alters the Spatial*

Proximity of Transmembrane Domain 7 to the Ligand Binding Pocket, 19th American Peptide Society Symposium - Understanding Biology Using Peptides, San Diego, CA, USA, 2005, Blondelle, S. E., Ed.; American Peptide Society: San Diego, **2005**; pp 357−358.

(64) Fillion, D.; Guillemette, G.; Leduc, R.; Escher, E. Photoprobe peptides to map the interactions of angiotensin II with its receptor AT1. *Adv. Exp. Med. Biol.* **2009**, *611*, 329–330.

(65) Rihakova, L.; Deraet, M.; Auger-Messier, M.; Perodin, J.; Boucard, A. A.; Guillemette, G.; Leduc, R.; Lavigne, P.; Escher, E. Methionine proximity assay, a novel method for exploring peptide ligand-receptor interaction. *J. Recept. Signal Transduct. Res.* **2002**, *22*, 297–313.

(66) Ballesteros, J. A.; Weinstein, H. *Integrated methods for the construction of three-dimensional models and computational probing of structure-function relations in G protein-coupled receptors*; Academic Press: San Diego, CA, 1995; pp 366−428.

(67) Fraker, P. J.; Speck, J. C., Jr. Protein and cell membrane iodinations with a sparingly soluble chloroamide, 1,3,4,6-tetrachloro-3a,6a-diphrenylglycoluril. *Biochem. Biophys. Res. Commun.* **1978**, *80*, 849–857.

(68) Wiener, H. L.; Reith, M. E. Determination of radioligand specific activity using competition binding assays. *Anal. Biochem.* **1992**, *207*, 58–62.

(69) Wiener, H. L.; Reith, M. E. Unknown radioligand specific activity. *Trends Pharmacol. Sci.* **1993**, *14*, 294–296.

(70) Sambrook, J.; Russell, D. W. Molecular Cloning: A Laboratory Manual; Cold Spring Harbor Laboratory Press, 2001; Vol 3, pp A8.40−A48.51.

(71) Schagger, H.; von Jagow, G. Tricine-sodium dodecyl sulfate-polyacrylamide gel electrophoresis for the separation of proteins in the range from 1 to 100 kDa. *Anal. Biochem.* **1987**, *166*, 368–379.

(72) Schagger, H. Tricine-SDS-PAGE. *Nat. Protoc.* **2006**, *1*, 16–22.